Available online at www.sciencedirect.com

SCIENCE DIRECT®

Journal of Molecular Catalysis A: Chemical 204–205 (2003) 561–569

JOURNAL OF MOLECULAR CATALYSIS A: CHEMICAL

www.elsevier.com/locate/molcata

Van der Waals interactions on acidic centres localized in zeolites nanocavities: a calorimetric and computer modeling study

V. Bolis[a,*], M. Broyer[a], A. Barbaglia[a], C. Busco[b], G.M. Foddanu[b], P. Ugliengo[b]

[a] *DiSCAFF, Università del Piemonte Orientale "A. Avogadro", Via Bovio 6, 28100 Novara, Italy*
[b] *Dipartimento di Chimica IFM, Università di Torino, Via P. Giuria 7, 10125 Torino, Italy*

Received 14 October 2002; received in revised form 18 January 2003; accepted 2 February 2003

Dedicated to Professor Renato Ugo on the occasion of his 65th birthday

Abstract

Adsorption enthalpies of CO, N_2 and Ar on H-BEA and H-MFI zeolites have been measured calorimetrically at 303 K in order to assess the energetic features of Lewis and Brønsted acidic sites. The interaction of the molecular probes with model clusters mimicking Lewis and Brønsted sites has been simulated at ab initio level, and a good agreement between the experimental and the calculated binding energies (BE) has been found. The combined use of the two different approaches has allowed to discriminate among the different interactions (Lewis, Brønsted and dispersive forces) contributing to the measured heat of adsorption. Confinement effects have been investigated on an all-silica MFI zeolite in order to measure the dispersive forces contribution due to the zeolite cavities. For the acidic zeolites both uptake and enthalpy changes correlate well with proton affinity and polarizability of the molecular probes. Whereas CO and N_2 single out contributions from Lewis and Brønsted acidic sites, Ar is only sensitive to *confinement effects*.

Keywords: Adsorption; Zeolites; Microcalorimetry; Ab initio calculations; Lewis acidity

1. Introduction

Proton-exchanged zeolites are widely used as solid-acid catalysts in many industrial processes [1]. Their Brønsted acidity is due to $\equiv Si(OH)^+Al^-\equiv$ species originated by the isomorphous substitution of some Si atoms by Al. A great deal of work has been devoted in the past decades to the characterization of such species, and much about the nature and properties of these sites is known [2,3], even if their precise quantitative characterization is not yet routinely available [4]. A far less understood feature of some zeolites (of which β-zeolite is a well known case [5,6]) is their ability to show Lewis acidity, in addition to the Brønsted one. At variance with the detailed knowledge of the Brønsted features, very little is known about the nature and structure of the Lewis sites.

The aim of the present work is to provide new insight in the structural and energetic features of the Lewis acidic sites in zeolites. To this purpose, the adsorption of Ar, N_2 and CO on zeolites of different structure and Si/Al ratio has been investigated by microcalorimetry at 303 K. H-β zeolite (BEA structure [7,8]) has been chosen owing to its richness in Lewis centres, mainly localized at the stacking faults between the two equally stable crystalline phases,

* Corresponding author. Tel.: +39-0321-689-842/845; fax: +39-0321-689-821.
E-mail address: bolis@pharm.unipmn.it (V. Bolis).

1381-1169/$ – see front matter © 2003 Elsevier Science B.V. All rights reserved.
doi:10.1016/S1381-1169(03)00339-X

whereas H-ZSM-5 zeolite (MFI structure [9]) has been chosen in that it mainly sports Brønsted acidic sites [10], even though it is well known that a variable amount of Al defects is always present in ZSM-5 materials [11]. An all-silica MFI zeolite (Silicalite [12]) with the same series of interconnected channels as H-ZSM-5 [13] has been chosen to gauge the contribution of the dispersive forces [14]. A non-porous system (δ-Al_2O_3) was also investigated as a prototype of Lewis acidic solid, characterized by the presence at the surface of coordinatively unsaturated *cus* Al^{III} ions [15,16].

In order to gauge the various contributions to the heats of adsorption, ab initio calculations of the binding energies (BE) of the probes with model clusters representative of both Lewis and Brønsted sites have also been performed. The measured enthalpy of adsorption ($q = -\Delta H_{ads}$) is indeed an intrinsically average value resulting from both the specific interaction of the molecular probes with Lewis and Brønsted centres, and the non-specific dispersive interactions with the zeolite walls (responsible of the so-called *confinement effect* [17,18]).

2. Experimental

2.1. Materials

(i) H-β zeolite (BEA, Si/Al = 9.8, Al/uc = 5.9), H-ZSM-5 (MFI, Si/Al = 15, Al/uc = 6.0), Na- and Al-free defective Silicalite (MFI Si/Al → ∞), kindly supplied by Polimeri Europa s.r.l., Centro Ricerche Novara Istituto G. Donegani, Novara, Italy; (ii) δ-Al_2O_3 (Alon-C, by Degussa). All samples have been *vacuum* activated ($p \leq 10^{-5}$ Torr, 14 h; 1 Torr = 133.3 Nm^{-2}) at either $T = 673$ K (H-ZSM-5 and Silicalite), $T = 873$ K (H-β) or $T = 1023$ K (δ-Al_2O_3) in order to achieve the maximum dehydration of the surface compatible with the stability of the structure.

2.2. Methods

2.2.1. Adsorption microcalorimetry

The heats of adsorption were measured at 303 K by a heat-flow microcalorimeter (Calvet C80, Setaram) in order to evaluate the enthalpy changes ($q = -\Delta H_{ads}$) related to the adsorption. A well-established stepwise procedure was followed [16,19]. The calorimeter was connected to a high vacuum ($p \leq 10^{-5}$ Torr) gas-volumetric glass apparatus, which enables to determine the adsorbed amounts (n_{ads}) and the integral heats (Q^{int}) evolved for small increments of the adsorptive. The calorimetric data are here reported either as *differential heats* ($q^{diff} = \delta Q^{int}/\delta n_{ads}$) or as *molar heats* ($[q]_p = [Q^{int}/n_{ads}]_p$), normalized to the uptake at the equilibrium pressure p. The q^{diff} curves reported in the plots are the derivatives of the Q^{int} versus n_{ads} polynomial functions (not reported for the sake of brevity) which best fit the equilibrium data obtained, whereas the experimental points are the partial molar heats of adsorption defined as ($\Delta Q^{int}/\Delta n_{ads}$). These latter quantities are obtained by the experimental $\Delta Q^{int}/\Delta n_{ads}$ versus n_{ads} histogram [19,20].

The complete reversibility of the process was checked by performing a second run after outgassing the sample overnight. The pressure was monitored by a transducer gauge (Ceramicell 0–100 Torr, Varian).

2.2.2. Molecular modeling

All calculations have been run at ab initio level using the B3-LYP functional on selected molecular clusters modeling the different sites. For Lewis sites, in order to mimic the different geometrical strains around the *cus* Al^{III} likely present in the real material, two different clusters (LSC and LLC) have been adopted (see Fig. 5 for details), whereas for the Brønsted site one Si atom has been replaced by Al in the faujasite unit cell (adopted because of its geometrical rigidity). The charge compensating acidic proton has been added to the most spatially available oxygen atom (see Fig. 6 for details). For calculations involving the LSC cluster, full B3-LYP/6–31 + G(d,p) geometry optimisation has been carried out, whereas for the LLC cluster, the ONIOM[B3-LYP/6–31 + G(d,p):MNDO] method [21] has been adopted to save computer resources. For the Brønsted site, either free or in interaction, full geometry optimisation with the ONIOM[B3-LYP/SVP:AM1] method has been carried out. The model regions, for both Lewis and Brønsted sites are shown as balls and sticks. When Ar is involved as a probe, neither AM1 nor MNDO can be used as low level methods in the ONIOM scheme, due to the lack of the corresponding parameters. Therefore, for the LLC case, the HF/3-21G method has been adopted as a low level, whereas for

the Brønsted site, due to its large size, only the model region has been used, keeping its geometry fixed at the optimised one for the free model, while manually minimizing the B3-LYP/6–31 + G(d,p) energy as a function of the H–Ar distance. For the ONIOM optimised structures, single point B3-LYP/6–31 + G(d,p) energy calculations have been carried out, from which binding energies, corrected for the basis set superposition error (BSSE), have been computed.

3. Results and discussion

3.1. Adsorption microcalorimetry

In Fig. 1 the differential heats of adsorption of CO on H-β zeolite are reported as a function of the adsorbed amounts, in comparison with H-ZSM-5, Silicalite and δ-Al_2O_3. In the inset of the figure the volumetric isotherms are shown. The interaction of CO with H-β is significantly larger (from both an energetic and a quantitative point of view) than that observed for the other systems, which in turn show remarkable differences. The q_0 value (differential heat extrapolated to zero coverage, representing the enthalpy change for the adsorption on the most energetic sites active in the early stage of the process) for H-β is ≈70 kJ/mol, compatible with a σ-coordination of CO on *cus* trigonal Al^{III} ions [16,22] and very close to the extrapolated q_0 value for the Lewis acidic prototype δ-Al_2O_3. The coverage attained for non-porous alumina is however dramatically lower than for β-zeolite ($n_{ads} \approx 20$ instead of ≈134 μmol/g, at $p_{CO} \approx 80$ Torr), suggesting that a major role is played by the presence of molecular-sized cavities, as witnessed also by the CO uptake on H-ZSM-5, which contains much less abundant Al defects than H-β.

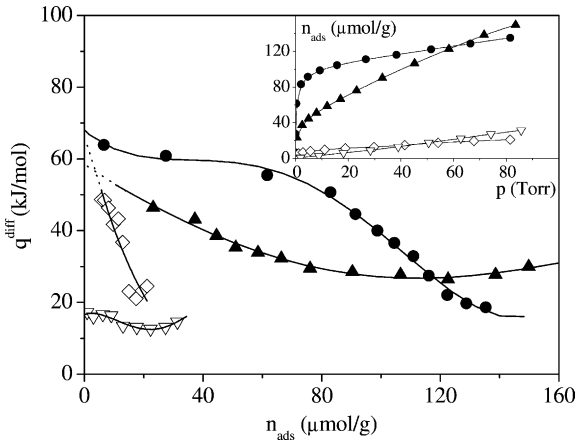

Fig. 1. Differential heats of adsorption (303 K) of CO on H-β (●) and H-ZSM-5 (▲) zeolites, on Silicalite (▽) and on δ-Al_2O_3 (◇) reported as a function of the adsorbed amounts. Inset: volumetric isotherms (adsorbed amounts vs. equilibrium pressure).

The enthalpies of adsorption cover a wide range of values from q_0 down to ≈20 kJ/mol for both H-β and δ-Al_2O_3, but in the case of alumina the heat values drop much more sharply. The heat value of 20 kJ/mol is very low for σ-coordination, but in the case of δ-Al_2O_3 at high p_{CO} the interaction is suspected to involve an endothermic step (which lowers the measured heat with respect to a plain σ-coordination, see [16,22]), whereas in the case of H-β zeolite at high p_{CO} the formation of H-bonded adducts on Brønsted sites (which involves a much lower energy of interaction) starts to prevail (vide infra). As far as the coverage increases, the heat of adsorption of CO for H-β zeolite remains almost constant at ≈60 kJ/mol over a relatively large coverage interval (≈80 μmol/g). This enthalpy value, still compatible with a σ-coordination process, indicates that on average 5 molecules of CO/100 Al atoms are σ-coordinated on *cus* Al^{III} sites. Conversely, heat values lower than ≈60 kJ/mol are assigned to the formation of H-bonded adducts on Brønsted ≡Si(OH)$^+$Al$^-$≡ sites.

As for H-ZSM-5, the extrapolated q_0 (≈60 kJ/mol) is higher than what expected for the sole formation of H-bonded adducts on Brønsted acidic sites confined in the pores, which should be close to 30 kJ/mol (as reported by Gorte and co-workers [23]). However, it has been demonstrated by IR spectroscopy (spectra not reported for brevity) that in the adopted H-ZSM-5 sample abundant *cus* Al^{III} ions able to σ-coordinate CO are present, which are responsible for the evolution of a heat comprised in the ≈60–30 kJ/mol interval. Beside this effect, the interaction of CO with H-ZSM-5 is mainly due to the formation of H-bonded adducts entrapped in the cavities of the microporous system. It is worth noting that the *confinement effect* due to the cavities is more pronounced for the 10-membered MFI than for the 12-membered BEA structure (as witnessed also by the adsorption of Ar, vide infra). At high coverage indeed, when the formation of H-bonded adducts

and the dispersive interactions prevail, the q^{diff} measured for H-β (≈20 kJ/mol) is lower than for H-ZSM-5 (≈30 kJ/mol).

The effect due to the presence of the nanocavities is energetically quantified by adsorbing CO on Silicalite for which a nearly constant heat of adsorption of ≈17 kJ/mol has been measured, in agreement with what found by Savitz et al. [24] at 195 K. The Na- and Al-free Silicalite studied in the present work is much more reactive than expected for a Silicalite exposing only virtually inert SiOSi bridges, in that it contains abundant hydroxylated species (*hydroxyl nests*), which are able to form H-bonded adducts with molecules, as described in [12,19]. The major role played by the walls of the pores in stabilizing the adducts formed is however witnessed by the fact that the interaction of CO with a "*perfect*" (i.e. free of hydroxylated defects) or a "*defective*" Silicalite (such as the present one) was found to be virtually the same (data not reported for brevity).

The shape of the volumetric isotherms varies according to the nature and the energetics of the processes occurring at the surface of the various samples examined. At the early stage of the process, the H-β isotherm is almost pressure-independent, grows steeply and at high pressure tends to saturate. At the opposite, the H-ZSM-5 isotherm initially grows smoothly, but at high equilibrium pressure instead of approaching the saturation keeps increasing steeply and crosses the H-β isotherm. This datum suggests that when the specific strong adsorption on Lewis sites is accomplished, the formation of H-bonded adducts (operative on both kind of zeolites) is favoured in the microporous system sporting the smallest cavities (MFI). Conversely, the Silicalite isotherm is strongly pressure-dependent (as typical of a process involving weak, non-specific interactions) and remains very low in the whole range of pressure examined. By contrast, the δ-Al_2O_3 isotherm, even if extremely low, exhibits a Langmuir-like shape similar to the one of H-β, as a consequence of the specific σ-coordination of CO on the *cus* Al^{III} sites.

In Fig. 2 the differential heats of adsorption of N_2 on H-β are reported as a function of the adsorbed amounts and compared with H-ZSM-5, Silicalite and δ-Al_2O_3 (volumetric isotherms in the inset of the figure). Also in this case the interaction of the probe with H-β is the most energetic, and the interaction with Silicalite

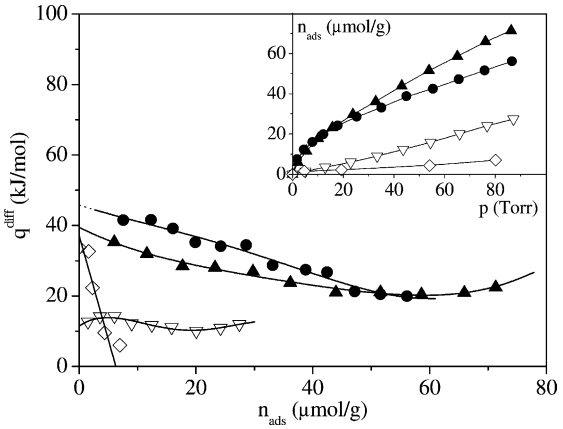

Fig. 2. Differential heats of adsorption (303 K) of N_2 on H-β (●) and H-ZSM-5 (▲) zeolites, on Silicalite (▽) and on δ-Al_2O_3 (◇) reported as a function of the adsorbed amounts. Inset: volumetric isotherms (adsorbed amounts vs. equilibrium pressure).

the least energetic. However, remarkable differences with respect to the interaction of CO are observed. The population of the sites sufficiently acidic to bind N_2 is much lower than those active towards CO, according to the PA values (476 and 582 kJ/mol for N_2 and CO, respectively). At $p = 80$ Torr, the amounts of N_2 adsorbed are only 53 μmol/g corresponding to ≈3.5 molecules/100 Al atoms (against 134 μmol/g for CO, i.e. ≈9 molecules/100 Al atoms).

Opposite to the CO case, the shape of N_2 isotherms is very similar for both H-β and H-ZSM-5 (in the early stage of the process they are virtually coincident) indicating that N_2 is a much less suitable probe to discriminate between Lewis and Brønsted sites. For Silicalite and δ-Al_2O_3 the interaction with N_2 is very scarce and heavily pressure-dependent. Again, the presence of nanocavities favours the adsorption of the probe on Silicalite with respect to a more acidic but non-porous solid.

Ar adsorption (which is very scarce, at the limit of detection) hardly discriminates among the different systems studied, as shown in Fig. 3, where the heats of adsorption are reported as a function of the adsorbed amounts (volumetric isotherms in the inset of the figure). All enthalpy values measured are quite low, but q^{diff} for H-β (16–7 kJ/mol) are somehow lower than for H-ZSM-5 (27–14 kJ/mol), which contains a population of Lewis acidic sites much less abundant than H-β (vide supra). This result suggests that the

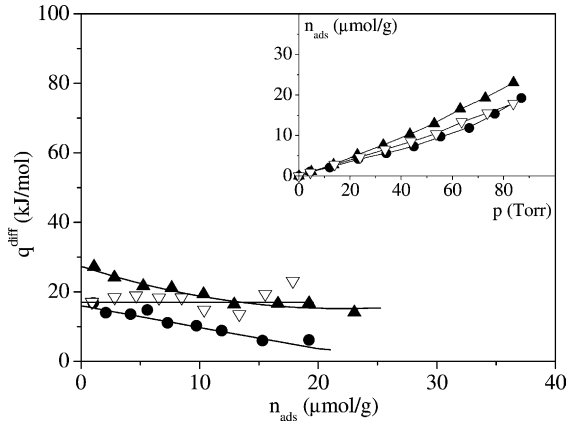

Fig. 3. Differential heats of adsorption (303 K) of Ar on H-β (●) and H-ZSM-5 (▲) zeolites and on Silicalite (▽) reported as a function of the adsorbed amounts. Inset: volumetric isotherms (adsorbed amounts vs. equilibrium pressure).

interaction of Ar (PA = 369 kJ/mol) with the zeolites is not specific for the Lewis or the Brønsted acidic sites, but involves only a non-specific interaction dominated by dispersive forces. Such forces are expected to be stronger on MFI systems, characterized by channels of smaller pore aperture than BEA. Indeed, the heat measured for Silicalite (≈16 kJ/mol) is intermediate between H-β and H-ZSM-5. *Confinement effects* are larger within the MFI framework than in BEA. The higher value of the q_0 for H-ZSM-5 compared to Silicalite is probably due to the stronger electrostatic field in the former, with some polarization contributions to the binding energy [25]. The adsorption on the Lewis acidic δ-Al_2O_3 is negligible, according to the lack of microporosity. The coverage attained is very small in all cases (according to the weak energetics of the process) and this fact represents the most severe limitation to the accuracy of the measurements. For instance, at $p = 80$ Torr only 17 μmol/g are adsorbed on H-β (i.e. ≈1 Ar atom/100 Al atoms).

In Fig. 4 the energetics of the adsorption of the three molecular probes are correlated to the basic strength of the molecules. The molar enthalpies of adsorption ($[q]_p = [Q^{int}/n_{ads}]_p$) measured at low and high pressure (10 and 80 Torr, a and b, respectively) are reported as a function of either the proton affinity (PA, kJ/mol) or the polarizability (α, $C^2\,m^2\,J$). The pressure of 10 Torr has been chosen because at this pressure the heat of adsorption of CO (the most specific

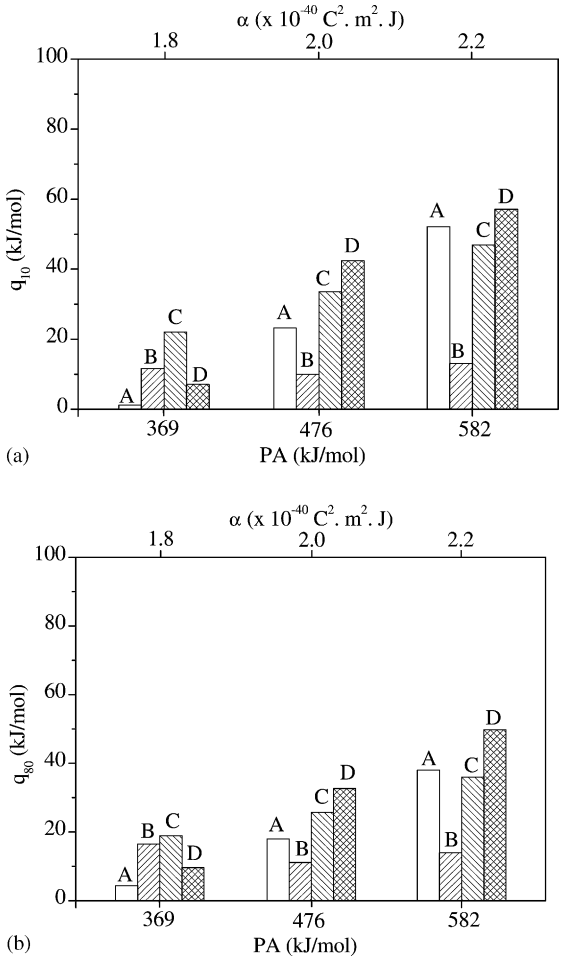

Fig. 4. Molar heats of adsorption ($[q]_p = [Q^{int}/n_{ads}]_p$) of CO, N_2 and Ar on H-β (D) and H-ZSM-5 (C) zeolites, Silicalite (B) and δ-Al_2O_3 (A) reported as a function of proton affinity (PA) and polarizability (α), at low equilibrium pressure ($p = 10$ Torr) (a) and high equilibrium pressure ($p = 80$ Torr) (b).

probe for Lewis acidic sites, as resulted by the present volumetric–calorimetric data) is dominated by the interaction with the Lewis sites. The pressure of 80 Torr has been chosen because at this stage of the process the heat measured is comprehensive of the whole phenomena. The energy of interaction of the probes increases as far as PA (or α) increases for the acidic systems (the two H-zeolites and δ-Al_2O_3), whereas it is grossly independent from the basic strength of the probe for the nominally non-acidic Silicalite. The same scenario is observed at both low and high equilibrium pressure.

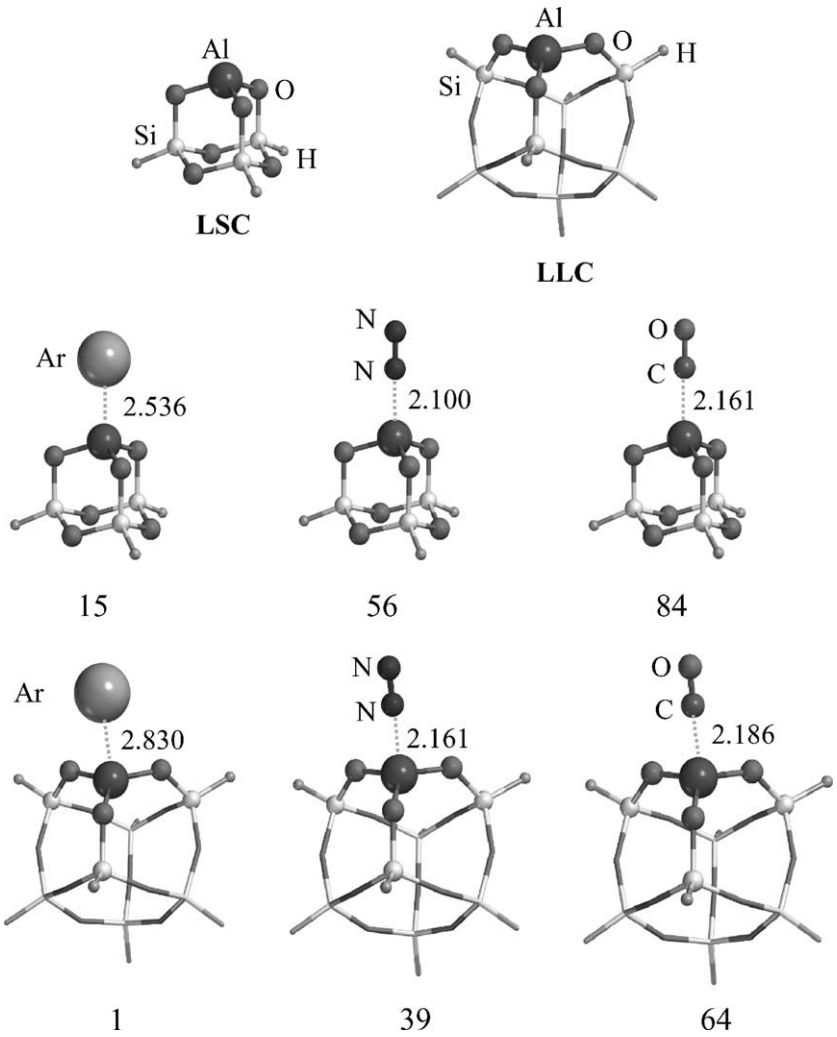

Fig. 5. Models of the Lewis site (LSC and LLC) both free and in interaction with the molecular probes. For LLC, the ONIOM model zone is depicted as balls and sticks. For each complex, the intermolecular distance (Å) and the corresponding BSSE corrected B3-LYP/6–31+G(d,p) binding energy value (kJ/mol) is reported.

For Ar adsorption on Lewis acidic δ-Al_2O_3 a value averaged on the highly scattered data measured[1] is reported for comparison. The low-pressure *molar heats* of adsorption of CO on H-β and H-ZSM-5 (for which at low p_{CO} the adsorption on Lewis sites is favoured) and on δ-Al_2O_3 (for which the adsorption involves only Lewis sites) are relatively close (q_{10} = 58, 49, 51 kJ/mol, respectively). This datum confirms that, as far as the Lewis acid–base interaction between *cus* Al^{III} sites and CO prevails, the energetics of the process is not very different in the various systems considered. However, the molar heat of 58 kJ/mol measured for H-β is significantly higher than for the other systems, suggesting that on β-zeolites the acidic strength of the Lewis sites is likely enhanced by the geometrical strain of the Al defects.

[1] The adsorbed amounts are very small in this case and thus the ratio $([Q^{int}/n_{ads}]_p = [q]_p)$ for the Ar/δ-Al_2O_3 interaction is not accurate enough.

3.2. Computational study

Figs. 5 and 6 show the optimised structures of the complexes formed between the probe molecules and, respectively, Lewis and Brønsted models. The relevant intermolecular distance and the BSSE corrected binding energy are indicated. As already anticipated, little is known about the structural and chemical nature of the Lewis sites in zeolites, and thus two different models have been studied (first row of Fig. 5) mimicking different geometrical constraints around the Al atom, in order to envisage different environment in the real material. The LSC cluster sports the highest sterical strain of the [AlO_3] moiety, the SiOAl angle being close to 110°. Because of that, the oxygen lone pairs can hardly be used to fill the Al unsatisfied valency, and result in an enhanced Lewis acidic strength with respect to the LLC model, in which a more relaxed geometrical environment is present (SiOAl angle around 145°). Indeed, the intermolecular distances computed for the complexes formed with the molecular probes are much shorter for the LSC cluster (second row of Fig. 5) than for the LLC one (third row), while the relevant binding energies are higher for the former with respect to the latter, according to the geometrical strain of the Al species. The BE increase along the series Ar < N_2 < CO for both models, in agreement with the PA (and α) values of the probes. The two sets of values for BE on LSC and LLC models can be assumed as a possible energy range to which the experimental energetic data can be compared. For instance, for CO adsorbed on the Lewis-rich H-β zeolite, the q_0 value (at vanishing coverage coordination on Lewis sites is supposed to prevail) is ≈70 kJ/mol, which falls in between the two computed values (64 and 84 kJ/mol, for LLC and LSC, respectively). The same holds for N_2 adsorption, in that q_0 is ≈45 kJ/mol, falling between LLC and LSC values (39 and 56 kJ/mol, respectively). For the Ar case, some limits in the modeling procedure become apparent. In this case, dispersive contributions to the differential heats of adsorption are the largest fraction of the binding (see the closeness of the experimental curves in Fig. 3). However, the computed BE does not include at all dispersive interactions. This is due, on the one hand, to the adopted B3-LYP functional, unable to cope with purely dispersive forces and, on the other hand, to the model cluster not including the silica walls responsible of the non-specific van

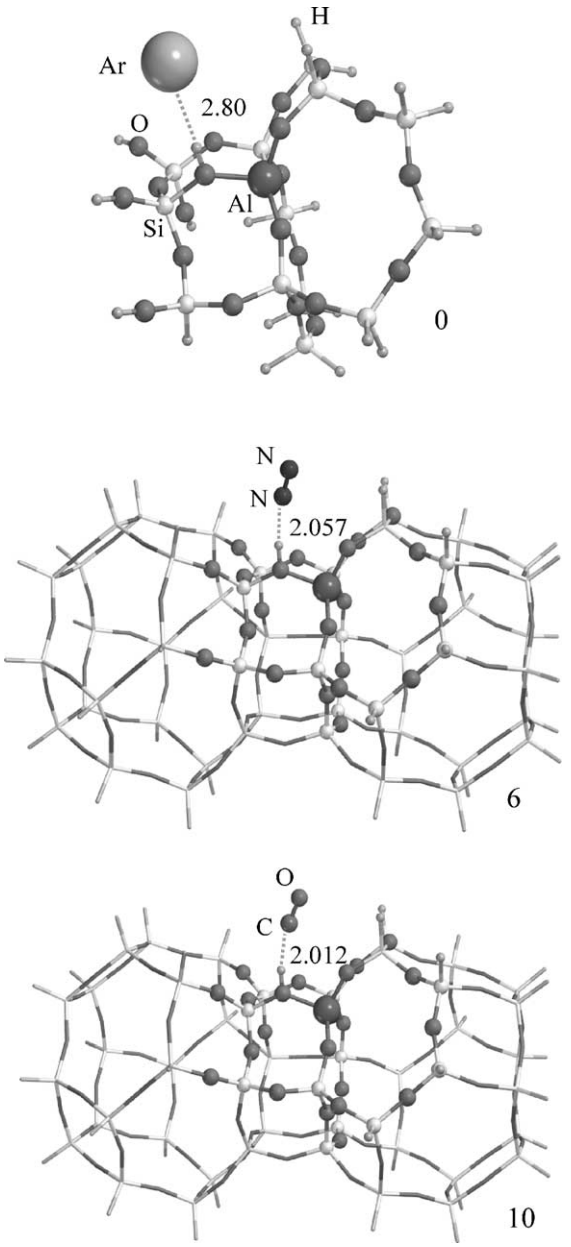

Fig. 6. Models of the Brønsted site in interaction with the molecular probes. For CO and N_2 cases, the ONIOM model zone is depicted as balls and sticks. For each complex, the intermolecular distance (Å) and the corresponding BSSE corrected B3-LYP/6–31 + G(d,p) binding energy value (kJ/mol) is reported.

der Waals forces. Indeed, the computed BE for Ar on the LLC model resulted in a mere 1 kJ/mol, whereas for LSC, the corresponding value of 15 kJ/mol is entirely due to the strong polarization of the Ar atom by the *cus* Al^{III} atom. Experiments (see Fig. 3) show that q_0 for the Lewis-rich H-β is close to that measured for Lewis-free Silicalite, indicating that either the LSC model has a too strong Lewis acidic strength if compared to the sites in the real material, or that the Lewis sites in the H-β zeolite are not easily accessible for Ar atoms (van der Waals radius of 1.9 Å).

The modeling study has been extended to the Brønsted site, the results of which have been shown in Fig. 6. The energy of interaction follows the same trend already found for the adsorption on the Lewis site, i.e. CO > N_2 > Ar. However, the BE are by far much lower than those computed for the Lewis site. BE values for CO and N_2 resulted in 10 and 6 kJ/mol, respectively, whereas for Ar the complex is virtually unbound, even if the Ar atom remains in the closeness of the Brønsted site because of the BSSE. These data strongly support the energy partition already proposed for the experimental values of the heats of adsorption. Indeed, for CO the difference in BE between the Lewis–LLC and the Brønsted site interaction (Δ(BE) = 54 kJ/mol) is maximum, in agreement with what indicated by the H-β and H-ZSM-5 q^{diff} versus coverage curves (see Fig. 1). For N_2, the difference between the two sites is less pronounced (Δ(BE) = 33 kJ/mol), in agreement with the similarity of the two experimental curves (see Fig. 2).

4. Conclusions

The adsorption of CO, N_2 and Ar on zeolites of different structure and Si/Al ratio has provided new insights on the structural and energetic features of Lewis acidic sites in zeolites. The adsorption enthalpies (measured calorimetrically at 303 K) correlate well with proton affinity and polarizability of the molecular probes, as well as with the binding energies calculated ab initio with model clusters mimicking Lewis *cus* Al^{III} acidic centres and Brønsted $\equiv Si(OH)^{+}Al^{-}\equiv$ sites. Dispersive forces responsible for *confinements effects* in zeolite nanocavities were found to play a major role in stabilizing the van der Waals adducts formed at the Lewis or Brønsted acidic sites (as well as on hydroxylated species on defective Silicalite). CO is the only probe which selectively discriminates between Lewis and Brønsted sites, particularly for H-β zeolite, sporting abundant Al^{III} defects. Ar was found to be very sensitive to *confinement effects*, and almost insensitive to specific interaction with the acidic sites.

Acknowledgements

This work was financially supported by the Italian MURST (cofin 2000, coordinated by Prof. A. Zecchina, Area 03: “Structure and reactivity of catalytic centres in zeolitic materials”). Dr G. Spanò and F. Rivetti (Polimeri Europa s.r.l., Centro Ricerche Novara Istituto G. Donegani, Novara, Italy) are greatly acknowledged for kindly supplying the microporous samples studied in the present work, and Prof. S. Bordiga (University of Torino, Italy) for fruitful discussions.

References

[1] A. Corma, Chem. Rev. 95 (1995) 559.
[2] A. Zecchina, C. Lamberti, S. Bordiga, Catal. Today 41 (1998) 169.
[3] R.J. Gorte, Catal. Lett. 62 (1999) 1.
[4] W.E. Farneth, R.J. Gorte, Chem. Rev. 95 (1995) 615.
[5] P.J. Kunkeler, B.J. Zuurdeeg, J.C. van der Waal, J.A. van Bokhoven, D.C. Koningsberger, H. van Bekkum, J. Catal. 180 (1998) 234.
[6] C. Pazè, S. Bordiga, C. Lamberti, M. Salvataggio, A. Zecchina, G. Bellussi, J. Phys. Chem. B 101 (1997) 4740.
[7] J.B. Higgins, R.B. LaPierre, J.L. Schlenker, A.C. Rohrman, J.D. Wood, G.T. Kerr, W.J. Rohrbaugh, Zeolites 8 (1988) 446.
[8] G.H. Kuehl, H.K.C. Timken, Microporous Mesoporous Mater. 35–36 (2000) 521.
[9] G.T. Kokotailo, S.L. Lawton, D.H. Olson, W.M. Meier, Nature (London) 272 (1978) 437.
[10] J.A. Dunne, M. Rao, S. Sircar, R.J. Gorte, A.L. Myers, Langmuir 12 (1996) 5896.
[11] M. Trombetta, G. Busca, S. Rossini, V. Piccoli, U. Cornaro, A. Guercio, R. Catani, R.J. Willey, J. Catal. 179 (1998) 581.
[12] S. Bordiga, I. Roggero, P. Ugliengo, A. Zecchina, V. Bolis, G. Artioli, C. Lamberti, J. Chem. Soc., Dalton Trans. (2000) 3921.
[13] E.M. Flanigen, J.M. Bennett, R.W. Grose, J.P. Choen, R.L. Patton, R.M. Kirchner, J.V. Smith, Nature 271 (1978) 512.
[14] J.A. Dunne, R. Mariwala, M. Rao, S. Sircar, R.J. Gorte, A.L. Myers, Langmuir 12 (1996) 5888.

[15] L. Marchese, S. Bordiga, S. Coluccia, G. Martra, A. Zecchina, J. Chem. Soc., Faraday Trans. 89 (1993) 3483.
[16] V. Bolis, G. Cerrato, G. Magnacca, C. Morterra, Thermochim. Acta 312 (1998) 63.
[17] R.J. Gorte, D. White, Microporous Mesoporous Mater. 35–36 (2000) 447.
[18] L. Yang, K. Trafford, O. Kresnawahjuesa, J. Sepa, R.J. Gorte, D. White, J. Phys. Chem. B 105 (2001) 1935.
[19] V. Bolis, C. Busco, S. Bordiga, P. Ugliengo, C. Lamberti, A. Zecchina, Appl. Surf. Sci. 7824 (2002) 1.
[20] V. Bolis, S. Maggiorini, L. Meda, F. D'Acapito, G. Turnes Palomino, S. Bordiga, C. Lamberti, J. Chem. Phys. 113 (2000) 9248.
[21] S. Dapprich, I. Komaromi, K.S. Byun, K. Morokuma, M.J. Frisch, J. Mol. Struct. (THEOCHEM) 461–462 (1999) 1.
[22] V. Bolis, G. Magnacca, C. Morterra, Res. Chem. Interm. 25 (1999) 25.
[23] S. Savitz, A.L. Myers, R.J. Gorte, J. Phys. Chem. B 103 (1999) 3687.
[24] S. Savitz, A.L. Myers, R.J. Gorte, Microporous Mesoporous Mater. 37 (2000) 33.
[25] H. Matsubashi, T. Tanaka, K. Arata, J. Phys. Chem. B 105 (2001) 9669.